*Inorg. Chem.* **2008**, *47*, 723–728


# Interface Reaction Route to Two Different Kinds of $CeO_2$ Nanotubes

**Guozhu Chen, Caixia Xu, Xinyu Song, Wei Zhao, Yi Ding,* and Sixiu Sun***

*Key Laboratory of Colloid and Interface Chemistry, Ministry of Education, School of Chemistry and Chemical Engineering, Shandong University, Jinan 250100, China*

Received September 20, 2007

$CeO_2$ nanotubes have been synthesized with a simple solid–liquid interface reaction route in the absence of any surfactants. Although the basic reaction principles are similar, two kinds of nanotubes with completely different morphologies and structures can be generated by slightly tuning the postprocessing conditions. The first formation involves employing $Ce(OH)CO_3$ nanorods as both the physical and chemical templates, and the other requires layered $Ce(OH)_3$ as an anisotropic intermediate species. During this process, NaOH and reaction temperature were demonstrated as the key factors responsible for the formation of $Ce(OH)_3$ intermediate and final $CeO_2$ nanotubes with well-defined structures. The structural details were provided by a combination of XRD, SEM, TEM, and HRTEM investigations. Catalytic measurement shows that both nanotubes are very active for CO oxidation, and at 250 °C, the conversion rates of $CeO_2$ nanotubes are 3 times higher than that of the bulk counterpart.

## Introduction

Tubular nanostructures have received significant research interest in recent years because they often exhibit intriguing properties, which may find diverse applications in areas such as catalysis, fuel cells, sensors, and separation.[1−4] So far, most examples require a layered or anisotropic crystal structure so that a certain degree of self-assembly may occur during the tubular structure formation.[5−9] Recently, synthesis of inorganic nanotubes from materials that do not possess a layered structure has also attracted considerable attention. Tubular structures including semiconductors, silicates, and metals have been successfully fabricated via a template-directed approach, concentration depletion method, or electrospinning technique.[10−15] Ceria ($CeO_2$) and ceria-based composite materials are important heterogeneous catalysts used in energy conversion and pollution control.[16−19] Recent advances in morphology-controlled synthesis of nanomaterials offered new opportunities of enabling materials with desired structural properties. For example, one-dimensional $CeO_2$ nanorods were found to be far more reactive than irregular nanoparticles.[20] Yu and co-workers[21] observed that spindle-like $CeO_2$ particles exhibited higher CO conversion catalytic activity than spherical and rodlike particles. Therefore, the synthesis of $CeO_2$ nanotubes with controllable structure features will be of particular significance.

Fluorite-structured $CeO_2$ does not have a layered structure, so it will require much more effort to synthesize $CeO_2$

* To whom correspondence should be addressed. Tel.: 86-531-88365432. Fax: 86-531-88366280. E-mail: ssx@sdu.edu.cn (S.S.). Tel.: 86-531-88366513. Fax: 86-531-88366280. E-mail: yding@sdu.edu.cn (Y.D.).

(1) Issues in nanotechnology. *Science* **2000**, *290*, 1523.
(2) Ma, R.; Bando, Y.; Golberg, D.; Sato, T. *Angew. Chem., Int. Ed.* **2003**, *42*, 1836.
(3) Nielsch, K.; Castano, F. J.; Ross, C. A.; Krishnan, R. *J. Appl. Phys.* **2005**, *98*, 034318.
(4) Bommel, K. J. C. V.; Friggeri, A.; Shinkai, S. *Angew. Chem., Int. Ed.* **2003**, *42*, 980.
(5) Tenne, R.; Margulis, L.; Genut, M.; Hodes, G. *Nature* **1992**, *360*, 444.
(6) Feldman, Y.; Wasserman, E.; Srolovitz, D. J.; Tenne, R. *Science* **1995**, *267*, 222.
(7) Chopra, N. G.; Luyken, R. G.; Cherrey, K.; Crespi, V. H.; Cohen, M. L.; Louie, S. G.; Zettl, A. *Science* **1995**, *269*, 966.
(8) Hacohen, Y. R.; Grunbaum, E.; Tenne, R.; Sloan, J.; Hutchison, J. L. *Nature* **1998**, *395*, 337.
(9) Nath, M.; Rao, C. N. R. *Angew. Chem., Int. Ed.* **2002**, *41*, 3451.
(10) Xia, Y.; Yang, P.; Wu, Y.; Mayers, B.; Gates, B.; Yin, Y.; Kim, F.; Yan, H. *Adv. Mater.* **2003**, *15*, 353.
(11) He, R. R.; Law, M.; Fan, R.; Kim, F.; Yang, P. *Nano Lett.* **2002**, *2*, 1109.
(12) Mayers, B.; Xia, Y. *Adv. Mater.* **2002**, *14*, 279.
(13) Matijevi, E. *Langmuir* **1994**, *10*, 8.
(14) Larsen, G.; Spretz, R.; Velarde-Ortiz, R. *Adv. Mater.* **2004**, *16*, 166.
(15) Loscertales, G.; Barrero, A.; Guerrero, I.; Cortijo, R.; Marquez, M.; Ganan-Calvo, A. M. *Science* **2002**, *295*, 1695.
(16) Jacobs, G.; Williams, L.; Graham, U.; Sparks, D.; Davis, B. H. *J. Phys. Chem. B* **2003**, *107*, 10398.
(17) Goubin, F.; Rocquefelte, X.; Whangbo, M. H.; Montardi, Y.; Brec, R.; Jobic, S. *Chem. Mater.* **2004**, *16*, 662.
(18) Varez, A.; Garcia-Gonzalez, E.; Sanz, J. *J. Mater. Chem.* **2006**, *16*, 4249.
(19) Monte, R. D.; Kaspar, J. *J. Mater. Chem.* **2005**, *13*, 633.
(20) Zhou, K. B.; Wang, X.; Sun, X. M.; Peng, Q.; Li, Y. D. *J. Catal.* **2005**, *229*, 206.
(21) Ho, C.; Yu, C. J.; Kwong, T.; Mak, A. C.; Lai, S. *Chem. Mater.* **2005**, *17*, 4514.

10.1021/ic701867f CCC: $40.75 
Published on Web 12/14/2007

nanotubes compared with layered $WS_2$ and $MoS_2$, where covalently bonded atoms form two-dimensional layers that are stacked together through van der Waals interaction.[22] However, it is worth noting that $Ce(OH)_3$ holds a layered structure, so the lamellar rolling of $Ce(OH)_3$ sheets may result in a tubular structure, which in turn may work as an anisotropic intermediate to form $CeO_2$ nanotubes under certain post-treatment conditions. Indeed, Han et al.[23] observed the coexistence of $CeO_{2-x}$ nanowires, nanoparticles, and nanotubes by boiling the mixed solution of cerium nitrate and ammonia hydroxide, followed by a long period of aging (45 days) at 0 °C. Tang et al.[24] reported that $Ce(OH)_3$ nanotubes could be synthesized through oxygen-free hydrothermal treatment of anhydrate $CeCl_3$, and $CeO_2$ nanotubes may be formed by controlled annealing of $Ce(OH)_3$ nanotubes in a reducing atmosphere. Recently, Zhou et al.[25] reported a facile synthesis of large-cavity $CeO_2$ nanotubes by etching $Ce(OH)_3$ nanotubes/nanorods with $H_2O_2$. In the present work, we report on the synthesis of $CeO_2$ nanotubes in alkaline solutions by employing $Ce(OH)CO_3$ nanorods as precursors. Although high-temperature decomposition−oxidation of $Ce(OH)CO_3$ has been reported to prepare $CeO_2$nanoparticles,[26−28] to the best of our knowledge, there is no report on solution-based preparation of $CeO_2$ by using $Ce(OH)CO_3$ as precursors. The interesting point of using $Ce(OH)CO_3$ nanorods relies on its slow kinetics of a solid−liquid interface reaction between hard-soluble $Ce(OH)CO_3$ nanorods and NaOH aqueous solution. In this reaction, "T" and "L" typed nanotubes can be obtained under different synthesis conditions, where "T" denotes the nanotubes which return to the templates, and "L" denotes the nanotubes which require layered $Ce(OH)_3$ as an intermediate. TEM and SEM images show that two kinds of $CeO_2$ nanotubes have distinctive structural features. Their catalytic properties were discussed, and both nanostructures showed great performance toward CO oxidation.

## Experimental Section

**Materials.** Cerious nitrate ($Ce(NO_3)_3{\cdot}6H_2O$, ≥99.0%), sodium hydroxide (NaOH, A.R. grade), urea ($CO(NH_2)_2$, A.R. grade), and commercial ceria ($CeO_2$, A.R. grade) were used as received from Sinopharm Chemical Reagent Co. Ltd.

**Synthesis of $Ce(OH)CO_3$ Precursors.** Rodlike $Ce(OH)CO_3$ precursors were synthesized by reacting cerium nitrate with urea according to the method reported by Chen et al.[29] In a typical experiment, 0.1736 g of $Ce(NO_3)_3{\cdot}6H_2O$ and 0.36 g of urea were added to 80 mL of water under vigorous magnetic stirring. The clear solution was charged into a 100 mL wide-mouthed jar which was closed and kept at 80 °C for 24 h. The solution was then air-cooled to room temperature. The obtained powder samples were centrifuged, washed with distilled water, and dried at 60 °C.

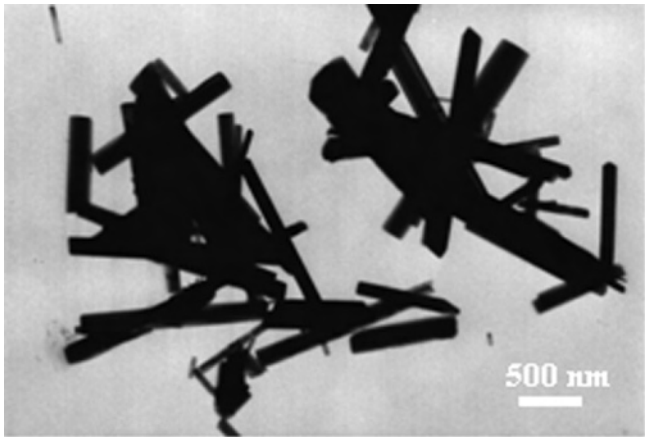


**Figure 1.** TEM image of the newly prepared $Ce(OH)CO_3$ precursors.

**Synthesis of "T" Nanotubes.** The $Ce(OH)CO_3$ nanorods obtained above (0.087 g) were re-dispersed into 20 mL of distilled water. Upon the addition of 2.4 g of NaOH, the mixture solution was stirred for 30 min and then kept at room temperature. After 4 days of aging, the light yellow precipitation was washed with $HNO_3$ (1 M), distilled water, and absolute ethanol sequentially, and then it was dried in a vacuum at 60 °C for 24 h.

**Synthesis of "L" Nanotubes.** The $Ce(OH)CO_3$ precursors (0.087 g) were re-dispersed into 20 mL of distilled water. After the addition of 0.48 g of NaOH, the mixture was transferred into a 30 mL stainless Teflon-lined autoclave and heated at 120 °C for 24 h. After the mixture was cooled to room temperature, yellow products were collected and washed several times with distilled water and absolute ethanol and then were dried in a vacuum at 60 °C for 24 h.

**Sample Characterization.** The samples were characterized by X-ray diffraction (XRD) on a Japan Rigaku D/Max-$\gamma$A rotating anode X-ray diffractometer equipped with graphite-monochromatized Cu Kα radiation ($\lambda = 1.54178$ Å) at a scanning rate of 0.02° $s^{-1}$ in the $2\theta$ range from 20° to 80°. The morphology and structure of as-synthesized $CeO_2$ nanotubes were characterized by field emission scanning electron microscopy (FESEM, JSM-6700F, 10 kV), transmission electron microscopy (TEM, JEOL 6300, 100 kV), and high-resolution transmission electron microscopy (HRTEM, JEM-2100, 200 kV). XPS spectra were recorded with a PHI 5300 X-ray photoelectron spectrometer using Al Kα radiation as the excitation source.

**Catalytic Activity Evaluation.** Catalytic activity was measured using a continuous flow fixed-bed microreactor at atmospheric pressure. In a typical experiment, the system was first purged with high-purity $N_2$ gas and then a gas mixture of $CO/O_2/N_2$ (1:10:89) was introduced into the reactor which contained 50 mg samples. Gas samples were analyzed with an online infrared gas analyzer (Gasboard-3121, China Wuhan Cubic Co.) which simultaneously detects CO and $CO_2$ with a resolution of 10 ppm. The results were further confirmed with a Shimadzu Gas Chromatograph (GC-14C).

## Results and Discussion

The simple reaction between cerium nitrate with urea generates rodlike $Ce(OH)CO_3$ with very high yield. Figure 1 shows a typical TEM image of these nanorod precursors. It can be seen that a majority of these nanorods have a diameter around 150−300 nm, with length typically larger

(22) Xiong, Y. J.; Mayers, T.; Xia, Y. N. *Chem. Commun.* **2005**, 5013.
(23) Han, W. Q.; Wu, L. J.; Zhu, Y. M. *J. Am. Chem. Soc.* **2005**, *127*, 12814.
(24) Tang, C.; Bando, Y.; Liu, B.; Golberg, D. *Adv. Mater.* **2005**, *17*, 3005.
(25) Zhou, K. B.; Yang, Z. Q.; Yang, S. *Chem. Mater.* **2007**, *19*, 1215.
(26) Qi, R. J.; Zhu, Y. J.; Cheng, G. F.; Huang, Y. H. *Nanotechnology* **2005**, 2502.
(27) Guo, Z. Y.; Du, F. L.; Li, G. C.; Cui, Z. L. *Inorg. Chem.* **2006**, *45*, 4167.
(28) Sun, C. W.; Sun, J.; Xiao, G. L.; Zhang, H. R.; Li, H.; Chen, L. Q. *J. Phys. Chem. B* **2006**, *110*, 13445.
(29) Chen, S. F.; Yu, S. H.; Yu, B.; Ren, L.; Yao, W. T.; Colfen, H. *Chem. Eur. J.* **2004**, *10*, 3050.

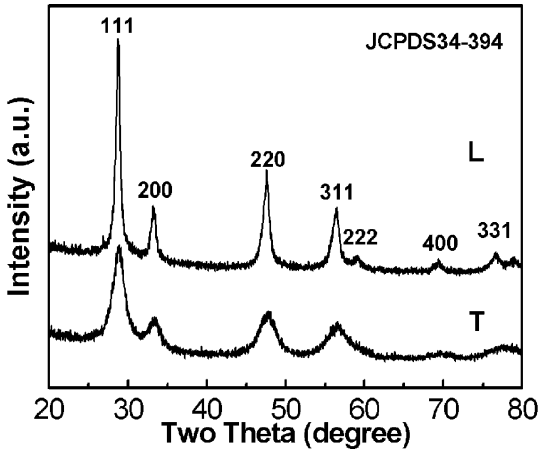


**Figure 2.** XRD patterns of "T"- and "L"-type nanotubes.

**Scheme 1.** Formation Processes of Two Different $CeO_2$ Nanotubes[a]

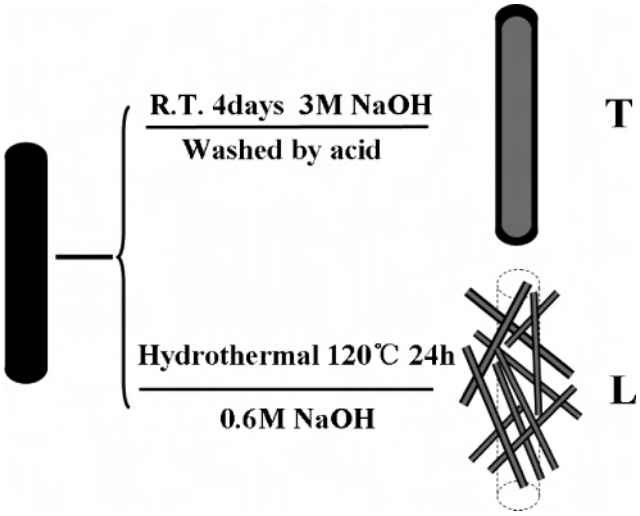


[a] L-nanotubes distribute randomly around $Ce(OH)CO_3$ nanorod precursors, and the dashed line in the figure denotes the precursor.

than 1 $\mu$m. X-ray diffraction shows that they are single-phase orthorhombic-structured $Ce(OH)CO_3$ (JCPDS 41-0013).

To fabricate $CeO_2$ nanotubes, two different processes were employed to treat $Ce(OH)CO_3$ nanorods. The first formation of $CeO_2$ nanotubes involves a process of a solid−liquid interface chemical reaction at room temperature and a subsequent removal of unreacted $Ce(OH)CO_3$ sacrificial templates by acid treatment. And the second formation requires a simple hydrothermal process without acid washing. A schematic illustration for the formation of $CeO_2$ nanotubes is depicted in Scheme 1. Figure 2 shows the X-ray diffraction patterns (XRD) of the obtained $CeO_2$ nanotubes, both of which can be indexed to a cubic fluorite-structured $CeO_2$ (JCPDS34-394). It is noted that the diffraction peaks of "T" are broader than those of "L", indicating that T type nanotubes contain smaller feature sizes as compared to L type. Based on the Scherrer equation, the average crystallite size can be estimated by analyzing the fwhm of the (111) diffraction peak, which is about 5.8 nm for T-type and 10 nm for L-type nanotubes. Considering that the properties of $CeO_2$ are related not only to its size and shape but also to its chemical composition, we probed the surface state of ceria

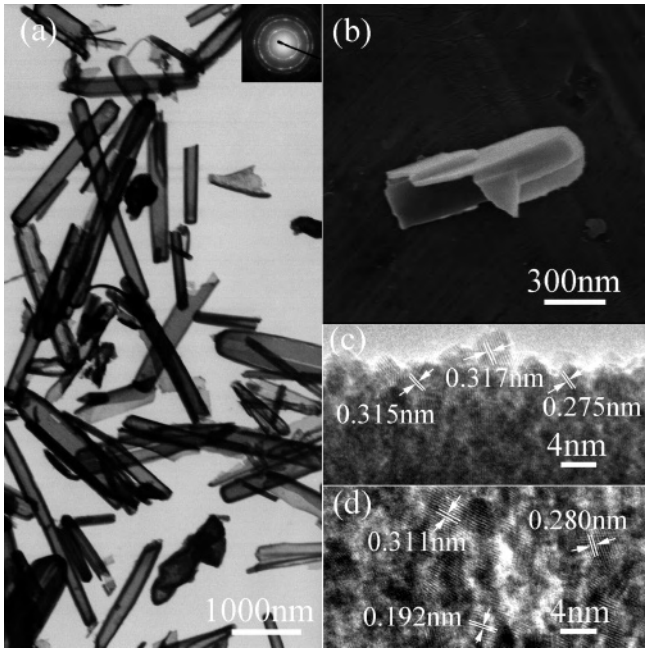


**Figure 3.** (a) Representative TEM image of T-nanotubes and its SAED pattern (inset); (b) SEM image of a ruptured T-nanotube; (c,d) HRTEM images from the shell and interior sites reveal the polycrystalline nature of the T-nanotube.

nanotubes by XPS (Figure S1). The relatively strong peaks at 901.8 and 882.8 eV can be attributed to the bonding energies of $Ce^{3+}$ $3d_{3/2}$ and $Ce^{3+}$ $3d_{5/2}$, indicating the existence of $Ce^{3+}$ on the surface of $CeO_2$ nanotubes.[30]

Figure 3a shows a typical TEM image of as-synthesized T-nanotubes. It can be seen that most particles hold a tubular structure with diameters in the range of 200−300 nm, which well resembles the shape and size of the $Ce(OH)CO_3$ nanorod templates (Figure 1). Figure 3b is an SEM image of a ruptured T-nanotube, which clearly shows a hollow interior of a tubular structure with shell thickness less than 15 nm. More detailed inspection with high-resolution TEM (HRTEM) imaging (Figure 3c and 3d) shows that the shell of T-nanotubes is constructed by small nanoparticles. These nanoparticles have a random orientation with an average size around 5 nm, which is consistent with the ring pattern in selected-area electron diffraction (inset in Figure 3a).

Figure 4a shows a TEM image of L-nanotubes. The sharp contrast between the edge and middle sites of these 1D structures is characteristic of a nanotube morphology observed by TEM. A majority of these tubes have a diameter around 30 nm and shell thickness $<4$ nm, which are markedly different from those of T-nanotubes. More interestingly, HRTEM imaging (Figure 4b) reveals continuous lattice fringes of cubic-structured $CeO_2$ over the whole nanotube, indicating those nanotubes have a single-crystal structure, which is further confirmed by the SAED pattern (inset in Figure 4a).

The formation of two distinctly different nanotubes from a similar system is very intriguing. We propose that an ion interface reaction between $Ce^{3+}$ and $OH^-$ is playing a crucial role in deciding the product structure. In our experiment,

(30) Wang, Z. L.; Quan, Z. W.; Lin, J. *Inorg. Chem.* **2007**, *46*, 5237.

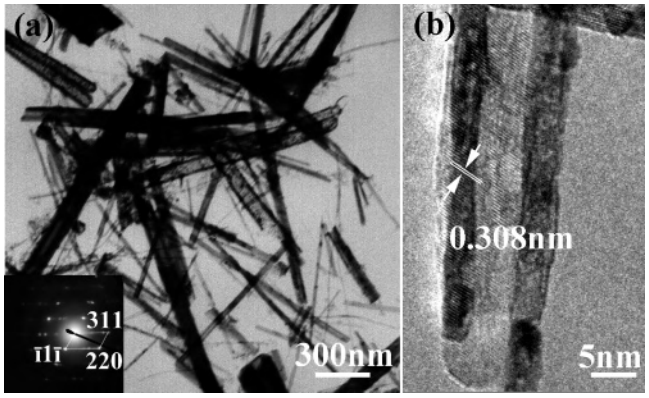


**Figure 4.** TEM (a) and HRTEM (b) images of L-nanotubes; inset in Figure 3a is a representative SAED of a single-crystalline L-nanotube.

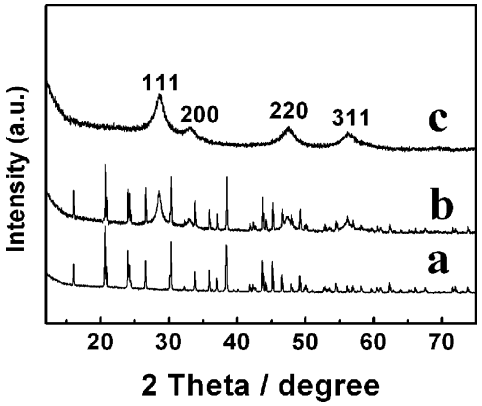


**Figure 5.** XRD patterns of (a) the newly prepared $Ce(OH)CO_3$; (b) the partially reacted $Ce(OH)CO_3$ after treatment with NaOH and exposure in air at room temperature for 4 days; and (c) T-type $CeO_2$ nanotubes synthesized after washing sample b with 1 M $HNO_3$.

$Ce(OH)CO_3$ was employed as the $Ce^{3+}$ source. As $OH^-$ is introduced into the system, the following reactions occur:

$$Ce(OH)CO_3(s) \leftrightarrow Ce^{3+} + OH^- + CO_3^{2-} \quad (1)$$

$$Ce^{3+} + 3OH^- \rightarrow Ce(OH)_3 \quad (2)$$

The increase of $OH^-$ concentration makes reaction (2) proceed toward the right, and eventually an interconnected $Ce(OH)_3$ shell forms around the external surfaces of $Ce(OH)CO_3$ nanorods. Meanwhile, higher pH value favors the oxidation of $Ce(OH)_3$, into $Ce(OH)_4$, which can be dehydrated and converted into $CeO_2$ under the drying process. This formation mechanism is similar to the case of hollow ZnO prepared by treating $Zn_5(CO_3)_2(OH)_6$ microspheres with KOH.[31]

Although the basic reaction principles are similar, the different postprocessing results in the formation of two different kinds of nanotubes. For T-nanotubes, the $Ce(OH)_3$ shell formed in the early stages can be converted into $CeO_2$ by aging with concentrated NaOH at room temperature for 4 days. Subsequently, the unreacted $Ce(OH)CO_3$ nanorod cores are washed away by diluted $HNO_3$. In a sense, here the $Ce(OH)CO_3$ nanorods act not only as chemical templates to provide the $Ce^{3+}$ source but also as physical templates to cast the morphology of the $Ce(OH)CO_3$ precursor. The structural evolution is also confirmed by XRD analysis (Figure 5) where one sees the coexistence of $Ce(OH)CO_3$ and $CeO_2$ before acid washing. For L-nanotubes, the hydrothermal condition favors the anisotropic growth of 1D $Ce(OH)_3$ structures rather than the formation of randomly oriented nanoparticles at room temperature as in the T-case. Subsequently, the lamellar rolling of $Ce(OH)_3$ nanosheets occurs to form tubular structures,[8] which will be transformed into $CeO_2$ nanotubes by hydroxide-assisted hydrothermal treatment. It has to be emphasized that although the resulted $CeO_2$ nanotubes have significantly different sizes and structures from those of precursors, here $Ce(OH)CO_3$ still works as a chemical template to provide the $Ce^{3+}$ source. And because the solid−liquid interface reaction initiates and proceeds preferentially on the surface of $Ce(OH)CO_3$ nanorods, one sees that the final 1D $CeO_2$ exhibits a bundle-like structure in a controlled fashion, where the original template shape can still be distinguished (Figure 6).

To further clarify the different mechanisms mentioned above, controlled experiments were carried out by using cube-shaped $Ce(OH)CO_3$ precursors rather than nanorods, and keeping other experimental conditions the same. And under the T-mechanism, we indeed obtained hollow cubes of $CeO_2$, while hydrothermal treating resulted in 1D nanowires and nanotubes (Figure 7). It is noted that the hollow $CeO_2$ nanocubes maintain the original shape of the precursor through the "T" process, while the thinner $CeO_2$ nanotubes distribute randomly around the precursor, although the precursor shape has changed. Regarding the shape evolution of $CeO_2$ under hydrothermal conditions, Yan and Xue[31] studied the formation of $CeO_2$ nanostructures by directly reacting $Ce(NO_3)_3$ with NaOH, and they suggested that the base concentration and the reaction temperature were two key factors responsible for the selective formation of $CeO_2$ nanostructures, such as nanopolyhedra, nanorods, and nanocubes. But they did not observe the nanotube structure. In our case, the reaction between hard-soluble rodlike $Ce(OH)CO_3$ and dilute NaOH has a much slower reaction kinetics, which may be particularly favorable for the formation of nanotubes under appropriate conditions. We have also studied the effects of these reaction parameters and found the higher the NaOH solution concentration and/or the reaction temperature, the easier the formation of $CeO_2$ nanorods rather than nanotubes (Figure 6). These results indicate that the dissolution/recrystallization rate drives the anisotropic growth of the hexagonal $Ce(OH)_3$ crystal nuclei.[32]

$CeO_2$ is an important three-way catalyst used in automobile exhaust systems; therefore, we studied the catalytic activity of $CeO_2$ nanotubes toward CO oxidation using a continuous flow fixed-bed microreactor. Figure 8 shows the activity profiles of both samples, along with that of a commercial $CeO_2$ sample for comparison. It is very clear that both nanotubes demonstrate much higher activity than bulk $CeO_2$.

(31) Yan, C. L.; Xue, D. F. *J. Phys. Chem. B* **2006**, *110*, 11076.

(32) Mai, H. X.; Sun, L. D.; Zhang, Y. W.; Si, R.; Feng, W.; Zhang, H. P.; Liu, H. C.; Yan, C. H. *J. Phys. Chem. B* **2005**, *109*, 24380.

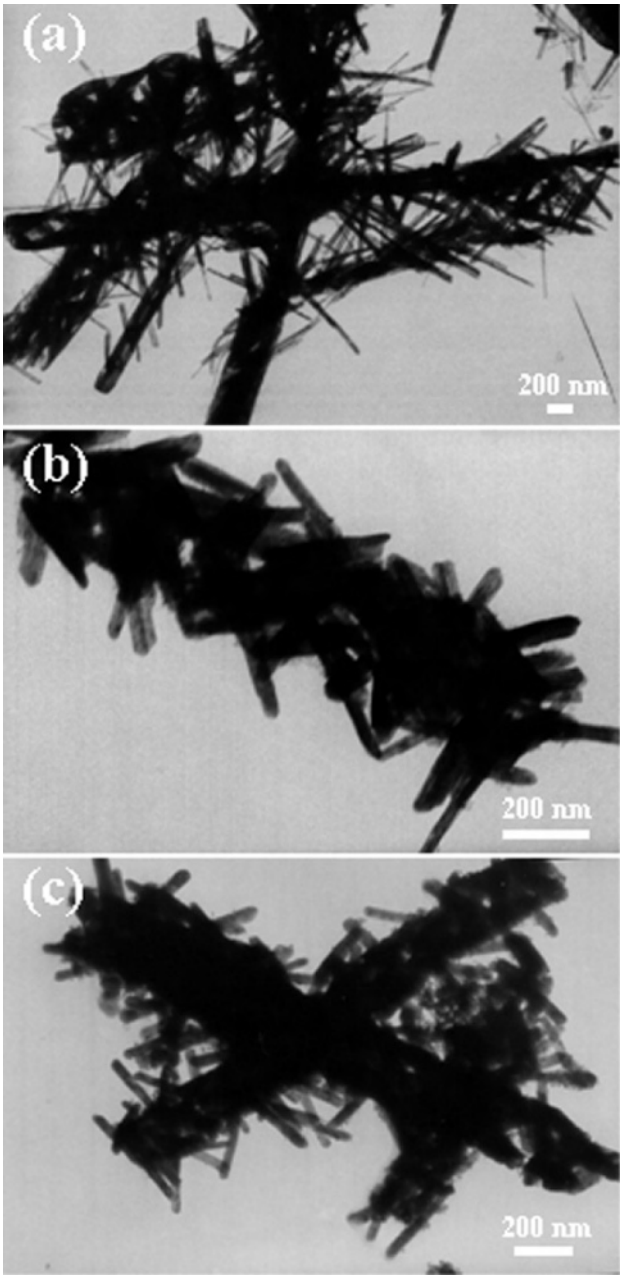


**Figure 6.** TEM images of $CeO_2$ samples synthesized under different hydrothermal conditions for 24 h: (a) 3 M NaOH, 120 °C; (b) 3 M NaOH, 180 °C; (c) 6 M NaOH, 180 °C.

At 250 °C, the conversion rates of nanotubes are 3 times higher than that of the bulk counterpart. And to achieve a similar conversion, the reaction temperature for nanotube samples can be at least 30 °C lower. It is generally accepted that the catalytic process is mainly related to the adsorption and desorption of gas molecules on the surface of catalyst. The interconnected hollow structure in our catalysts enables better contact with the gas molecules; therefore, they reasonably exhibit better performance. It is very interesting to find that although T-type nanotubes have much larger diameters, both samples are similarly active for CO oxidation. This is probably due to the fact that T-nanotubes are polycrystalline in nature with an actual grain size around 5 nm, which is very close to the shell thickness of L-nanotubes. Considering that the thermal stability of the catalyst is critical

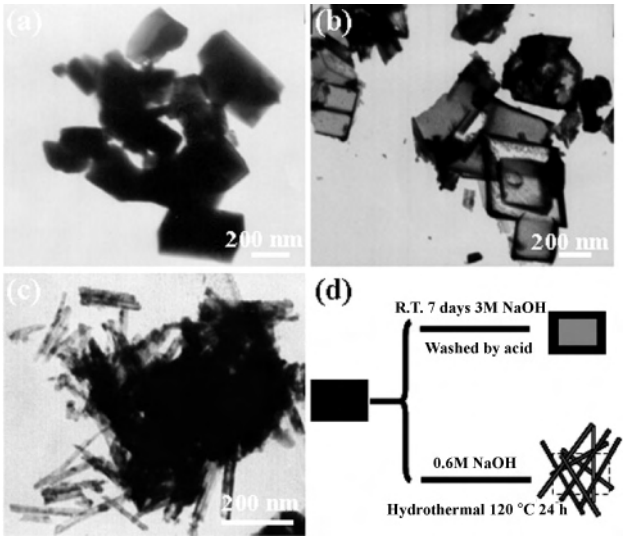


**Figure 7.** TEM images of (a) cube-shaped $Ce(OH)CO_3$ precursor; (b) hollow cubes obtained under T-mechanism; (c) "L" nanotubes/nanowires, treated under hydrothermal conditions; (d) schematic illustration of the formation of different $CeO_2$ hollow structures.

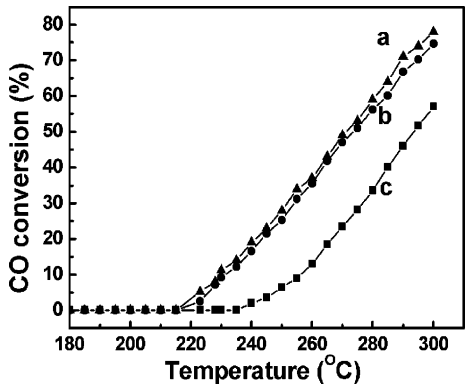


**Figure 8.** CO conversion as a function of temperature for the as-prepared $CeO_2$: "T"-nanotubes (line a); "L"-nanotubes (line b); commercial ceria powder (line c).

for practical applications, we annealed ceria nanotube samples at 400 °C for 4 h and then compared their catalytic activities with unannealed ones. And we found that annealing at such a high temperature had very little influence on their catalysis performance toward CO oxidation (Figure S3). In addition, TEM observation confirmed that, after catalysis reactions, both nanotubes retain their original tubular morphology very well (Figure S4), which is further evidence of $CeO_2$ nanotubes' excellent thermal stability.

## Conclusions

In conclusion, we successfully fabricated two kinds of $CeO_2$ nanotubes with distinctive structures and morphologies by using $Ce(OH)CO_3$ nanorods as precursors. Direct mixing of $Ce(OH)CO_3$ nanorods with NaOH solution at room temperature followed with a long period of aging and acid treatment generates polycrystalline $CeO_2$ nanotubes which well resemble the size and morphology of the precursor nanorods. And hydrothermal treatment of $Ce(OH)CO_3$ with dilute NaOH at a mild temperature (120 °C) produces single-crystal $CeO_2$ nanotubes with significantly smaller diameters. Despite their apparent difference, both nanotubes are in-

volved in the same solid−liquid interface reaction, where hard-soluble $Ce(OH)CO_3$ nanorods act as chemical and/or physical templates. The reaction conditions significantly influence the reaction velocity, the morphology of $Ce(OH)_3$ intermediates, and the structure features of final $CeO_2$ products. Interestingly, those two kinds of nanotubes show similar and better catalytic performance on CO oxidation than bulk $CeO_2$, possibly due to their comparable dimension in structure unit (T-type nanotubes have larger apparent sizes, but are polycrystalline.) Our method mentioned here may be applied to the fabrication of other metal oxides nanotubes. And more importantly, the method of tailoring the reaction kinetics to produce different nanotubes represents a new concept of nanostructure fabrication.

**Acknowledgment.** This work was supported by the National Science Foundation of China (50601015), the National 863 (2006AA03Z222) and 973 (2005CB623601, 2007CB936602) Program Projects of China, and the State Education Ministry's NCET Program (NCET-06-0580). Y.D. is a Tai-Shan Scholar supported by Shandong Province (2006BS04018).

**Supporting Information Available:** TEM image and XRD pattern of the commercial ceria, XPS spectra of $CeO_2$ nanotubes, and thermal stability of $CeO_2$ nanotubes (PDF). These materials are available free of charge via the Internet at http://pubs.acs.org.

IC701867F